Polymer Journal (2019) 51:471–480
https://doi.org/10.1038/s41428-018-0162-3

ORIGINAL ARTICLE

Viscoelasticity of poly(ethylene glycol) in aqueous solutions of potassium sulfate: a comparison of quartz crystal microbalance with conventional methods

Xiaoxue Wu[1] · Ziliang Zhao[1] · Yu Kang[1] · Xiangling Ji[1] · Yonggang Liu[1]

Received: 14 September 2018 / Revised: 3 December 2018 / Accepted: 4 December 2018 / Published online: 9 January 2019

Abstract

The viscoelasticity of poly(ethylene glycol) (PEG) in aqueous solutions with different concentrations of potassium sulfate (K_2SO_4) was studied by quartz crystal microbalance with dissipation (QCM-D), after coating a rigid supported lipid bilayer of 1,2-dioleoyl-*sn*-glycero-3-phosphocholine on the silicon oxide substrate. The obtained viscoelastic properties of PEG in K_2SO_4 solutions agree well with the Zimm model predictions for linear polymer chains. With increasing K_2SO_4 concentration, the excluded volume exponent ν of PEG decreased from 0.565 in water to 0.55 in 0.19 mol/L K_2SO_4, and 0.50 in 0.43 mol/L K_2SO_4. The solvent quality gradually worsened for PEG with increasing K_2SO_4 concentration, which was verified by decreases in the polymer intrinsic viscosity and the corresponding Mark–Houwink exponent. The high-frequency characteristic of QCM-D makes it possible to directly study the viscoelasticity of polymer solutions in a low-viscosity solvent, which is complementary to conventional rheometers working at low frequency.

Introduction

The dynamics of polymer chains in solutions or melts can be studied by measuring their viscoelastic properties in oscillatory shear flows at certain frequencies, which can probe the motion of whole chains or chain segments with the corresponding relaxation times [1, 2]. The typical upper frequency for conventional rheometers is approximately 100 Hz, which limits the application of such instruments in polymeric systems with sufficiently large relaxation times, usually for high-molecular-weight polymers with a large fluid viscosity. Time-temperature superposition has been employed to extend the frequency in a limited range by tuning the fluid viscosity via temperature [1]. It is, however, not applicable for aqueous polymer solutions because the viscosity of water weakly depends on temperature and the temperature range in which water acts as a good solvent for the studied polymers is limited. In some cases, a large amount of inert sugars can be added to the aqueous polymer solution to slow down the dynamics of the polymer chains by increasing fluid viscosity [3–5]. On the other hand, the classical theories on polymer dynamics in solutions and melts predict various scaling behaviors at high frequencies, which contain rich information about the relaxation mechanism of the polymeric fluid [6–9]. Therefore, it is crucial to directly measure the high-frequency viscoelasticity of polymer solutions, which provides important insight into their structure and dynamics.

Instruments based on torsional resonators, which was pioneered by Mason [10], have been used to study the viscoelasticity of polymer solutions up to hundreds of kHz [11–13]. Microrheological techniques based on the measurement of the motion of tracer particles in fluids, such as quasielastic light scattering (QELS) and diffusing wave spectroscopy (DWS) [14, 15], have been developed to measure the viscoelasticity of polymer solutions up to frequencies of 100 kHz but are not applicable to dilute polymer solutions. Very recently, we reported the viscoelasticity measurement of aqueous polymer solutions at megahertz frequency by quartz crystal microbalance with dissipation (QCM-D) [16]. In the report, the perturbations arising from polymer adsorption on the crystal resonator were eliminated by coating the resonator with a rigid and inert supported lipid bilayer (SLB), and the viscoelastic properties of poly

✉ Yonggang Liu
yonggang@ciac.ac.cn

[1] State Key Laboratory of Polymer Physics and Chemistry, Changchun Institute of Applied Chemistry, Chinese Academy of Sciences, 130022 Changchun, China

(ethylene glycol) (PEG) of different molecular weights in pure water were obtained from the shifts in the resonance frequency and the energy dissipation factor. The QCM-D method is proven to be a rapid and accurate way to study the viscoelasticity of aqueous polymer solutions at high frequency. This method only requires a small amount of samples, which is especially promising for costly or rare biological samples. It should be noted that biomacromolecules are often dissolved in an aqueous buffer containing salts. It is therefore necessary to study the feasibility of the QCM-D technique for polymer solutions in the presence of salts, especially in systems where the salt plays an important role in determining the conformation and dynamics of the polymer chains.

Here, we report the measurement of the viscoelasticity of aqueous PEG solutions containing different concentrations of potassium sulfate using QCM-D at high frequencies of 5-65 MHz. The effect of potassium sulfate concentration on polymer viscoelasticity is studied and compared with conventional measurements by an Ubbelohde viscometer and a rotational rheometer.

Materials and methods

Materials

The lipid of 1,2-dioleoyl-*sn*-glycero-3-phosphocholine (DOPC) was obtained from Avanti Polar Lipids, Inc. (Alabaster, Alabam, USA) and used without further purification. PEGs with different weight average molecular weights (M_ws) of 200, 400, 600, 1000, 1400, 2000, 4000, 6000, 8000, 10,000, 20,000, and 35,000 were purchased from Sigma-Aldrich and were desiccated under vacuum to a constant weight before experiments. The polydispersities (M_w/M_ns) of all PEG samples were less than 1.1, according to gel-permeation chromatography measurements. Three polyethylene oxides (PEOs) samples, synonymous with PEG, with higher molecular weights of 116,000, 278,000, and 443,000 were purchased from Polymer Laboratories, Ltd. Analytical-grade sodium chloride (NaCl) and potassium sulfate (K_2SO_4) were obtained from Sigma. Ultrapure water produced by a Sartorius water purification system with a resistivity of 18.2 MΩ·cm was used for solution preparations.

Viscoelasticity via QCM-D

The viscoelasticity of aqueous PEG solutions is measured by QCM-D after coating the resonator surface with an inert layer, which is provided by the rupture of liposomes to form a rigid SLB on the silicon oxide substrate. More details of the experimental procedure can be found elsewhere [16].

The liposomes were prepared by the extrusion method [16]. Briefly, a DOPC solution in chloroform was transferred into a continuously rolled vial, and the organic solvent was completely removed by evaporation with a gentle stream of nitrogen gas, followed by 3 h of vacuum pumping. An aqueous solution containing 150 mM NaCl was added to the vial to dissolve the dried lipid film upon gentle vortexing. The solution was then extruded 31 times through a 100 nm polycarbonate membrane with a mini-extruder (Avanti Polar Lipids, Inc.) to produce large unilamellar vesicles (LUVs). The average diameter of the obtained liposomes was 128 ± 2 nm with a narrow size distribution, according to dynamic light scattering measurements on a Malvern Nano ZS90 Zetasizer. Vesicle suspensions were kept at 4 °C and diluted to a lipid concentration of 0.1 mg/mL prior to use.

The QCM-D experiments were carried out at 24 ± 0.02 °C on a Q-Sense E4 system (Biolin Scientific, Sweden) [17]. Before mounting into the flow module, the AT-cut quartz crystal sensors with a fundamental resonance frequency of 4.95 MHz were cleaned twice with the following procedure: soaked in a 2% SDS solution for 30 min, rinsed with ultrapure water, blow-dried with nitrogen gas and exposed to an ultraviolet (UV)/ozone cleaner for 15 min [18]. The experiments were then performed in exchange mode by pumping at least 1.0 mL degassed sample solution into the 40 µL chamber at a fluid flow rate of 100 µL/min. The shifts in the resonant frequency Δf_n and the energy dissipation factor ΔD_n of the sensors were monitored simultaneously at multiple harmonics (overtone numbers $n = 1, 3, 5, 7, 9, 11, 13$).

The measurements started by forming a rigid and inert SLB on the sensor, which was produced by the rupture of DOPC liposomes facilitated in an aqueous solution containing 150 mM NaCl. After establishing the baseline with the 150 mM NaCl solution, the DOPC vesicle solution was pumped into the chamber to form the SLB on the resonator surface, followed by again rinsing with the 150 mM NaCl solution. The chamber fluid was exchanged to pure water before the aqueous solution of PEG in pure water or in different concentrations of K_2SO_4 was pumped into the chamber. Aqueous PEG solutions of different molecular weights were introduced into the chamber one by one, and a sufficient amount of water was pumped in between to rinse the SLB surface.

The relationship between the frequency shift Δf_n and the mass Δm of a thin and rigid film adsorbed onto the sensor is described by the Sauerbrey equation [19]:

$$\Delta m = -\frac{(\rho_q \mu_q)^{1/2}}{2f_0^2}\frac{\Delta f_n}{n} = -C\frac{\Delta f_n}{n} \quad (1)$$

where f_0 is the fundamental resonance frequency of the sensor (4.95 MHz), ρ_q is the density of quartz (2.648 g/cm^3), μ_q is the

shear modulus of the crystal (2.947×10^{11} g cm^{-1} s^{-2}), and C is the mass sensitivity constant (18.0 ng cm^{-2} Hz^{-1} at $f_0 = 4.95$ MHz). For Sauerbrey films, the frequency shift Δf_n is proportional to the overtone number n, and the dissipation shift $\Delta D_n \approx 0$. However, a soft and viscous adlayer will dissipate energy and damp the sensor oscillation. In this case, one can obtain information about the stiffness of the adlayer from the shift in the energy dissipation factor, which is defined as the energy dissipated per oscillation divided by the total energy stored in the oscillator.

For an oscillating quartz resonator in contact with a Newtonian fluid, the frequency shift and the dissipation shift arising from the presence of the fluid are [20–23]:

$$-\frac{\Delta f_n}{n} = n^{-1/2} f_0^{3/2} \left(\frac{\eta_l \rho_l}{\pi \mu_q \rho_q} \right)^{1/2} \tag{2}$$

and

$$\Delta D_n = 2 n^{-1/2} f_0^{1/2} \left(\frac{\eta_l \rho_l}{\pi \mu_q \rho_q} \right)^{1/2} \tag{3}$$

where η_l and ρ_l are the fluid viscosity and density, respectively. Therefore, the QCM-D measurement of a Newtonian fluid on a nonadsorbing resonator provides the fluid viscosity if its density is accurately measured.

For a viscoelastic fluid in contact with the quartz resonator [24–26], its complex-valued viscosity is related to the frequency shift and the dissipation shift for the dynamic viscosity

$$\eta'(\omega) = -\frac{\pi \rho_q \mu_q}{\rho_l f_n} \frac{\Delta f_n \cdot \Delta \Gamma_n}{f_0^2} \tag{4}$$

and the storage viscosity

$$\eta''(\omega) = \frac{1}{2} \frac{\pi \rho_q \mu_q}{\rho_l f_n} \frac{\Delta \Gamma_n^2 - \Delta f_n^2}{f_0^2} \tag{5}$$

where $\Delta \Gamma_n = \Delta D_n f_n / 2$ is the shift of the half-bandwidth, with $f_n = n f_0$ the frequency at each overtone n. Thereby, the QCM-D measurement of a viscoelastic fluid on a nonadsorbing resonator leads to its complex viscosities and shear moduli. It should be noted that the viscoelastic properties of the fluids are obtained at megahertz frequencies, $\omega = 2\pi f_n$.

Viscometry and rheometry

The viscosities of PEG solutions in pure water and different concentrations of K_2SO_4 were measured at 24 ± 0.1 °C by using an Ubbelohde viscometer with an efflux time of 243.0 s for pure water. Huggins and Kraemer plots were used to determine the intrinsic viscosity [η] of PEG. The density of each solution was measured at 24 ± 0.01 °C on a DMA 4500 M density meter (Anton Paar) with a resolution of 5×10^{-5} g/mL.

Linear viscoelastic measurements of PEG solutions were conducted on an ARES-G2 (TA Instruments) rheometer with a cone-and-plate geometry (with a cone radius of 25 mm and a cone angle of 2°) kept at 24 ± 0.1 °C. Frequency sweep measurements were performed at small amplitudes (<10%) to measure the storage and loss moduli, $G'(\omega)$ and $G''(\omega)$, as functions of the angular frequency, ω, between 2 and 500 rad/s. Shear-rate sweep measurements were performed to measure the viscosities of PEG solutions at shear rates that ranged from 5 to 500 s^{-1}.

Results and Discussion

Formation of a rigid supported lipid bilayer on the resonator

The formation of a SLB on a silicon oxide substrate was monitored by QCM-D, as shown in Fig. 1. After establishing the baseline with a 150 mM NaCl aqueous solution for approximately 5 min, the solution of DOPC liposome was pumped into the chamber at 7.0 min, and the observed decrease in the resonance frequency and increase in the energy dissipation factor were due to the adsorption of liposomes on the hydrophilic substrate. The frequency shifts, $\Delta f_n/n$, decreased to values between −61 and −36 Hz (the value was different for each overtone) at 10.5 min, before the signals reached a plateau value of −24.5 Hz (the value was the same for all harmonics) after 14.0 min. The corresponding dissipation shifts, ΔD_n, reached n-dependent maxima of approximately 7.0×10^{-6} before stabilizing at n-independent values of $0.1–0.2 \times 10^{-6}$. Such evolutions in the shifts of both resonant frequency and energy dissipation factors indicate the rupture of adsorbed soft liposomes to form a rigid SLB on the silicon oxide substrate, which agrees well with previous experimental and theoretical studies [16–18, 27–32]. The nonfouling nature of the SLB was employed to impede the nonspecific adsorption of samples on the sensor, which allowed for the fluid viscoelastic properties to be probed by QCM-D, as shown below.

Viscosity of potassium sulfate solutions

After forming the DOPC SLB on the silicon oxide substrate, the adsorption behavior of K_2SO_4 solutions on the SLB was subsequently studied at salt concentrations c_s between 0.1 and 0.6 mol/L. The resonance frequency and the energy dissipation factor for all 7 harmonics were monitored as the K_2SO_4 solution was pumped into the chamber, followed by rinsing with water. Figure 2a shows a

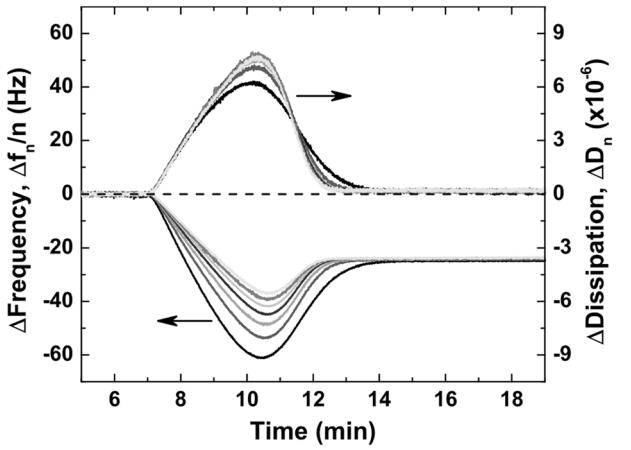

Fig. 1 QCM-D monitoring of the resonance frequency shifts $\Delta f_n/n$ and energy dissipation shifts ΔD_n during the formation of the DOPC SLB on a silicon oxide substrate. The frequency signals from bottom to top are for overtone numbers $n = 1, 3, 5, 7, 9, 11, 13$. The corresponding dissipation signal at each overtone is shown in the same color as the frequency. The black dashed line is a guide to the eyes with a value of 0 for the baseline

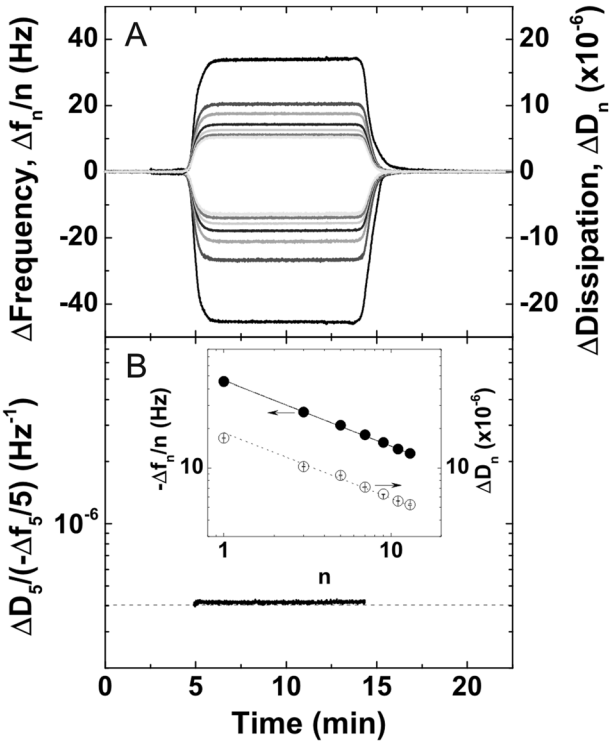

Fig. 2 A typical QCM-D measurement for a 0.39 mol/L K_2SO_4 aqueous solution on the DOPC SLB. **a** The resonance frequency shifts $\Delta f_n/n$ and the energy dissipation shifts ΔD_n for all harmonics as a function of time. The frequency signals from bottom to top are for overtone numbers $n = 1, 3, 5, 7, 9, 11, 13$. The corresponding dissipation signal at each overtone is shown in the same color as the frequency. **b** The ratio of the dissipation shift to the frequency shift for the 5th overtone, $\Delta D_5/(-\Delta f_5/5)$, as a function of time. The dashed line is the theoretical value of $2/f_0$ for Newtonian fluids. The inset shows the dependence of the frequency shift $-\Delta f_n/n$ and the dissipation shift ΔD_n on the overtone number n for the 0.39 mol/L K_2SO_4 aqueous solution. The solid and dashed lines are fittings to the data with a scaling exponent of $-1/2$

typical QCM-D measurement for a 0.39 mol/L K_2SO_4 aqueous solution on the DOPC SLB. The shifts in the resonance frequency and the energy dissipation factor induced by the K_2SO_4 solution disappeared as soon as they were rinsed away by water, indicating no irreversible adsorption. The ratio of the dissipation shift to the frequency shift, $\Delta D_n/(-\Delta f_n/n)$, was close to the theoretical value of $2/f_0 = 4.04 \times 10^{-7}\,\mathrm{Hz}^{-1}$ for Newtonian fluids (Fig. 2b). The values of $-\Delta f_n/n$ and ΔD_n were plotted as functions of the overtone number n, both showing the scaling laws of $-\Delta f_n/n \sim n^{-1/2}$ and $\Delta D_n \sim n^{-1/2}$ (inset of Fig. 2b). One can calculate the viscosity of the K_2SO_4 solution via eqs. (2) and (3) once the solution density is measured by a density meter. As shown in Fig. 3, the obtained viscosity of the K_2SO_4 solution agrees very well with the viscosity measured by a viscometer and the data in reference [33]. Therefore, forming a rigid SLB on the quartz resonator does not prevent it being a sensor for fluid viscosity. Instead, the bilayer served as a nonadsorbing interface to prevent nonspecific adsorption between the bare silicon oxide substrate and the solutions in the chamber, and the resonator can be used to measure the viscosity of the Newtonian fluids.

Viscoelasticity of PEG solutions in the presence of potassium sulfate

The viscoelasticity of aqueous PEG solutions in 0.19, 0.43, and 0.57 mol/L K_2SO_4 was studied by QCM-D. In aqueous PEG solutions, increasing the salt concentration decreases the lower consulate temperature, and the magnitude of this decrease depends on the nature of the salt according to the Hofmeister series [34–36]. For potassium sulfate, a strongly hydrated salt, the theta temperature of PEG decreases significantly with salt concentration. The theta temperature of PEG in 0.45 mol/L K_2SO_4 is ~35 °C, and an extrapolation to a theta temperature of 24 °C leads to a K_2SO_4 concentration of 0.53 mol/L [36]. Therefore, the above solvents are good, nearly theta and bad solvents for PEG/PEO. Indeed, it was found that in the 0.57 mol/L K_2SO_4 aqueous solution, although PEG samples with $M_w \leq 35{,}000$ were soluble, PEO samples with the highest M_w of 116,000, 278,000, and 443,000 were no longer soluble at a concentration of 2.0%, indicating a bad solvent condition in vicinity of the theta point. Fig. 4a shows a typical QCM-D measurement for dilute aqueous solutions of 2.0% PEG of different molecular weights in the 0.19 mol/L K_2SO_4 solution on the DOPC SLB. No irreversible adsorption of the PEG solution on the SLB was found in the studied molecular weight range. The ratio $\Delta D_n/(-\Delta f_n/n)$ for PEG with

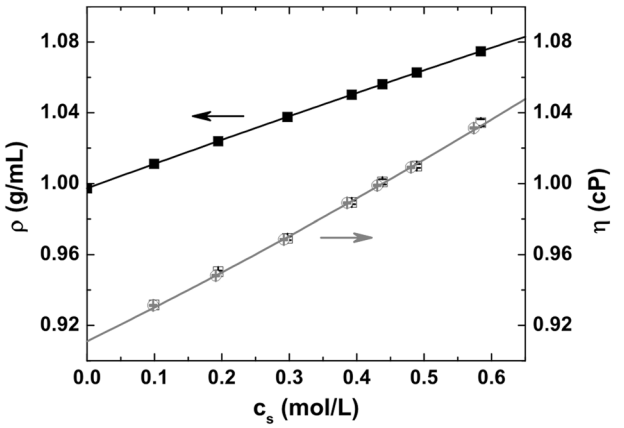

Fig. 3 Concentration dependence of the density (solid squares) and viscosity obtained by QCM-D (open squares) and a viscometer (open circles) of aqueous solutions of K_2SO_4 at 24 °C. The solid lines are fits to $\rho = \rho_0 + a_1 c_s + a_2 c_s^2$, with $\rho_0 = 0.99730$ g/mL, $a_1 = 0.13915$, and $a_2 = -0.01115$ for the density, and $\eta = \eta_0 + b_1 c_s + b_2 c_s^2$, with $\eta_0 = 0.911$ cP, $b_1 = 0.18759$, and $b_2 = 0.03515$ for the viscosity

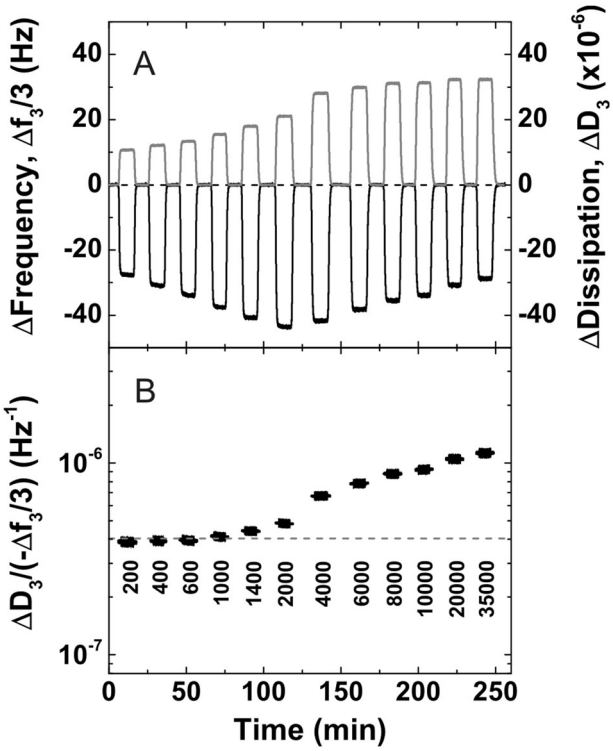

Fig. 4 QCM-D signals for a series of aqueous solutions of 2.0% PEG of different molecular weights containing 0.19 mol/L K_2SO_4 exposed to the DOPC SLB. The signals from left to right are for PEG with molecular weights of 200, 400, 600, 1000, 1400, 2000, 4000, 6000, 8000, 10,000, 20,000 and 35,000. **a**, **b** are the frequency shift $\Delta f_3/3$ (black curve) and the dissipation shift ΔD_3 (red curve), and their ratio $\Delta D_3/(-\Delta f_3/3)$, respectively. The red dashed line is the theoretical value of $\Delta D_3/(-\Delta f_3/3) = 2/f_0$ for Newtonian fluids

molecular weights 200, 400, 600, and 1000 is close to the theoretical value of $2/f_0 = 4.04 \times 10^{-7}$ Hz^{-1} for Newtonian fluids, and it increased with molecular weight to 1.1×10^{-6} Hz^{-1} for PEG-35000 (Fig. 4b). Therefore, the elastic property of PEG solutions becomes stronger for PEG of higher molecular weight.

In Fig. 5, the values of $-\Delta f_n/n$ and ΔD_n are plotted as functions of the normalized frequency $\omega\tau$ for 2.0% PEG/PEO aqueous solutions containing 0.19 mol/L K_2SO_4. Here, the frequency is normalized by the sample's Zimm relaxation time τ, as given by [9]:

$$\tau = 0.325 \frac{\eta_s \overline{R}^3}{k_B T} \tag{6}$$

where k_B is the Boltzmann constant, and $\overline{R}$ is the end-to-end distance of polymer with $\overline{R} = 6^{1/2} R_g$. The radius of gyration R_g can be obtained from the molecular weight according to the scaling relation $R_g \sim M_w^{\nu}$. Here, we use the relation R_g (nm) $= 0.0202 \times M_w^{0.58}$ for high-M_w PEG/PEO in 0.19 mol/L K_2SO_4 [37–39], while the relation R_g (nm) $= 0.0355 \times M_w^{0.50}$ obtained from light scattering and intrinsic viscosity measurements at theta condition [39, 40] was employed for all PEG/PEO samples in 0.43 and 0.57 mol/L K_2SO_4. The latter was also used for PEG samples with $M_w < 2000$ in 0.19 mol/L K_2SO_4, which are ideal chains with a negligible excluded volume, according to previous experiments and the coarse-grained simulation [16, 41, 42]. Both $-\Delta f_n/n$ and ΔD_n increased with molecular weight in the low-M_w region but behaved differently in the high-M_w region: a peak for $-\Delta f_n/n$ was observed, followed by a decrease to a plateau value at $M_w \geq 35{,}000$, while ΔD_n continuously increased with M_w to a plateau value at $M_w \geq 35{,}000$. It should be noted that both the frequency shift $-\Delta f_n/n$ and the dissipation shift ΔD_n became lower with increases in the overtone number n. Their scaling laws with frequency $\omega\tau$ (and overtone number n) showed a decrease in the exponents from $-1/2$ for low-M_w PEGs with $\omega\tau \ll 1$ to -0.76 for high-M_w ones with $\omega\tau \gg 1$, indicating a crossover from Newtonian to non-Newtonian behavior with increasing molecular weight. These observations are similar to previous results of PEG in pure water [16], indicating that the elastic properties of PEG in 0.19 mol/L K_2SO_4 get stronger at either increasing M_w or higher frequency. Fig. 6 compares the values of $-\Delta f_n/n$ and ΔD_n for PEG in aqueous solutions of different K_2SO_4 concentrations to those for PEG in the pure water. It is found that these curves had the same trend, and an increase in the absolute values of $-\Delta f_n/n$ and ΔD_n with increasing concentrations of K_2SO_4 was observed. The latter is due to the increase in the viscosity and density of the K_2SO_4 aqueous solution compared to those of pure water.

Using eqs. (4) and (5), we calculated the dynamic viscosity η' and storage viscosity η'' of PEG/PEO in aqueous K_2SO_4 solutions obtained from QCM-D. The shear moduli

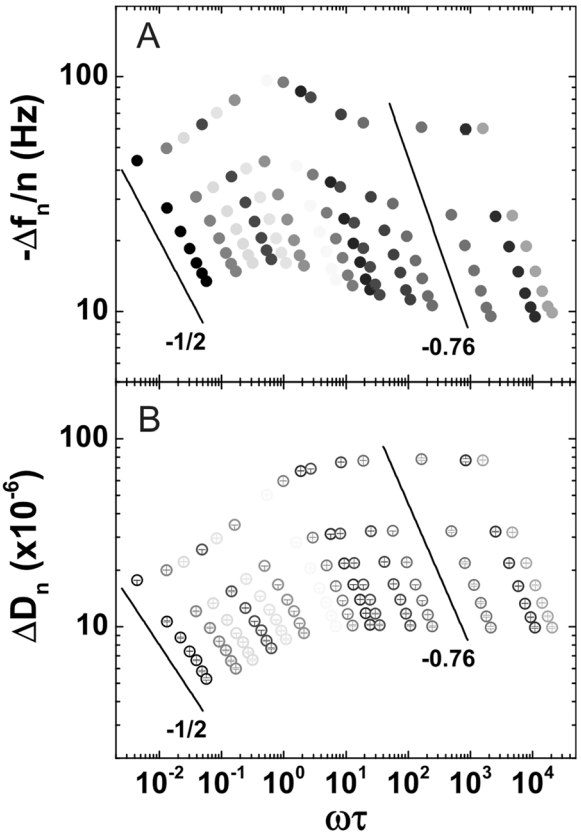

Fig. 5 Dependence of **a** the frequency shift $-\Delta f_n/n$ and **b** the dissipation shift ΔD_n on the normalized frequency $\omega\tau$ for a 2.0% PEG/PEO aqueous solution containing 0.19 mol/L K_2SO_4 on an SLB of DOPC. The data from left to right are for PEG/PEO with molecular weights of 200, 400, 600, 1000, 1400, 2000, 4000, 6000, 8000, 10,000, 20,000, 35,000, 116,000, 278,000, and 443,000. The solid lines serve as guides to the eye with scaling exponents of −1/2 for low-M_w PEG and −0.76 for high-M_w PEG/PEO

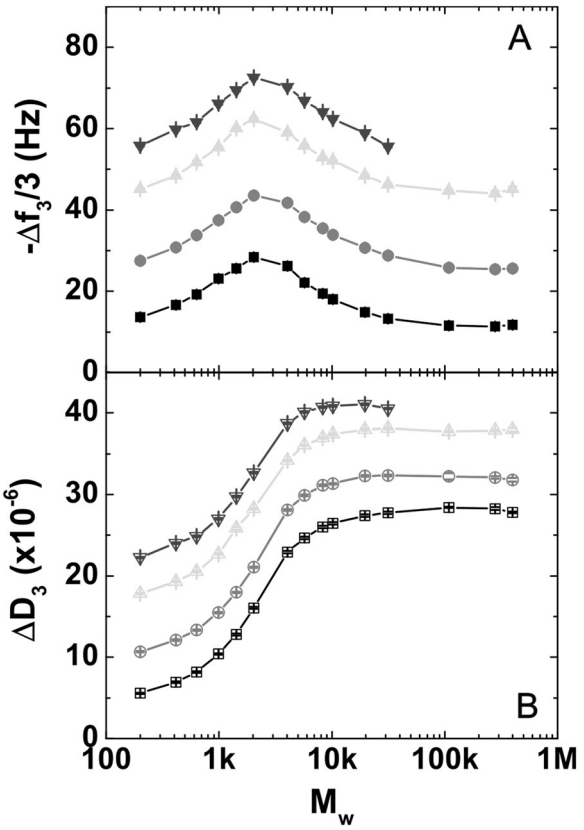

Fig. 6 The molecular weight dependence of **a** the frequency shift $-\Delta f_3/3$ and **b** the dissipation shift ΔD_3 for 2.0% PEG/PEO in pure water (squares), 0.19 mol/L K_2SO_4 (circles), 0.43 mol/L K_2SO_4 (upward triangles), and 0.57 mol/L K_2SO_4 (downward triangles) on an SLB of DOPC

attributed to the polymer can then be calculated via $G' = \omega\eta''$ and $G'' = \omega(\eta' - \eta_s)$, where G' is the storage modulus, G'' is the loss modulus, and η_s is the solvent viscosity. In Fig. 7, we plot the reduced storage modulus $G'M_w/(cRT)$ and reduced loss modulus $G''M_w/(cRT)$ as functions of $\omega\tau$ for all PEG/PEO samples in 0.19 mol/L and 0.43 mol/L K_2SO_4, respectively. Here, c is the polymer mass concentration, R is the gas constant, T is the absolute temperature, and τ is the Zimm relaxation time. For comparison, we also plot the Zimm model predictions of the reduced storage and loss moduli for dilute solutions of linear polymer chains [43];

$$\frac{G'M_w}{cRT} = \frac{\omega\tau \sin[(1-1/(3\nu))\arctan(\omega\tau)]}{\left[1+(\omega\tau)^2\right]^{(1-1/(3\nu))/2}} \quad (7)$$

$$\frac{G''M_w}{cRT} = \frac{\omega\tau \cos[(1-1/(3\nu))\arctan(\omega\tau)]}{\left[1+(\omega\tau)^2\right]^{(1-1/(3\nu))/2}} \quad (8)$$

It can be seen that the reduced shear modulus data for all PEG/PEO samples collapsed to single curves covering the $\omega\tau$ range between 10^{-2} and 10^4, which are very close to the Zimm model predictions with $\nu = 0.55$ in 0.19 mol/L K_2SO_4 and $\nu = 0.50$ in 0.43 mol/L K_2SO_4. In the region of $\omega\tau \ll 1$, the scaling exponents were 2.0 for $G'M_w/(cRT)$ and 1.0 for $G''M_w/(cRT)$. While in the region of $\omega\tau \gg 1$, both moduli had the same scaling exponent of $1/(3\nu)$, whose values were approximately 0.60 in 0.19 mol/L K_2SO_4 and 0.67 in 0.43 mol/L K_2SO_4. The former and latter values are in excellent agreement with the theoretical Zimm model of linear polymer chains in a good solvent and a theta solvent, respectively. The excluded volume exponent for PEG in 0.19 mol/L K_2SO_4, $\nu = 0.55$, was slightly smaller than the value of 0.565 for PEG in pure water [16], indicating that 0.19 mol/L K_2SO_4 is still a good solvent for PEG. In 0.43 mol/L K_2SO_4, the excluded volume exponent of $\nu = 0.50$ indicated a state close to the theta condition. In 0.57 mol/L K_2SO_4, a bad solvent, only PEG samples with $M_w \le 35000$ were soluble, and the obtained reduced shear modulus data were nearly the same as those for PEG in 0.43 mol/L

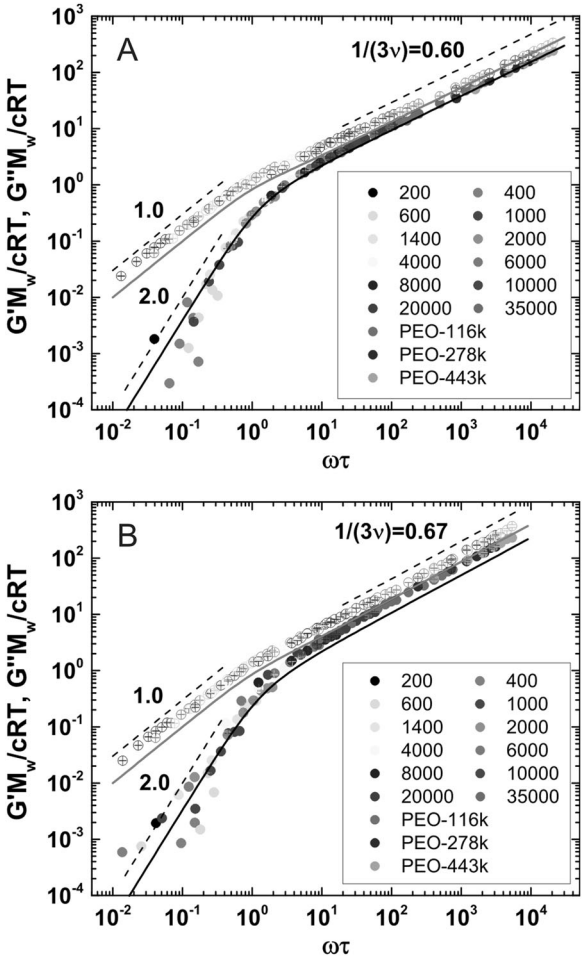

Fig. 7 Reduced storage modulus $G'M_w/(cRT)$ (solid symbols) and loss modulus $G''M_w/(cRT)$ (open symbols) for all PEG/PEO samples in **a** 0.19 mol/L and **b** 0.43 mol/L K_2SO_4 aqueous solutions. The solid curves are the predictions of the Zimm model with the excluded volume exponents $\nu = 0.55$ in (**a**) and $\nu = 0.50$ in (**b**). The dashed lines are guides to the eyes with the theoretical scaling exponents of 2.0 for $G'M_w/(cRT)$ and 1.0 for $G''M_w/(cRT)$ in the region of $\omega\tau \ll 1$ and $1/(3\nu)$ for both moduli in the region of $\omega\tau \gg 1$

K_2SO_4, agreeing with the Zimm model prediction for linear polymer chains in a theta solvent with an excluded volume exponent of $\nu = 0.50$.

For PEG with $400 \le M_w \le 2000$, in the region of $\omega\tau \ll 1$, the molecular weight dependence of the storage modulus $G' \sim M_w^{6\nu-1}$ and the loss modulus $G'' \sim M_w^{3\nu-1}$ led to the same value of $\nu = 0.50$ in aqueous solutions containing different concentrations of K_2SO_4 because these polymer chains were smaller than the thermal blob size and the excluded volume effect was not appreciable. For PEG with $M_w \ge 8000$, in the region of $\omega\tau \gg 1$, the frequency dependencies according to $G'M_w/(cRT) \sim (\omega\tau)^{1/(3\nu)}$ and $G''M_w/(cRT) \sim (\omega\tau)^{1/(3\nu)}$ led to the estimation of the excluded volume exponent ν for each sample, and the results are plotted as a function of molecular weight in Fig. 8 for PEG in all solvents. With increasing K_2SO_4 concentration, the excluded volume exponent in the high-M_w limit decreased from 0.565 in water (a good solvent) to 0.55 in 0.19 mol/L K_2SO_4 (a good solvent) and 0.50 in 0.43 mol/L K_2SO_4 (a near-theta solvent). Therefore, the viscoelastic properties of PEG solutions in K_2SO_4 at different concentrations can be obtained from the QCM-D measurement, which acts as a microrheometer working in the oscillation shear mode at high frequency.

Comparison with conventional viscometry and rheometry

The viscosities of PEG solutions in pure water and aqueous solutions containing different concentrations of K_2SO_4 were measured with a capillary viscometer. Fig. 9 shows the concentration dependence of the relative viscosities of PEG-35000 and PEG-600 in these solvents. The relative viscosities of PEG-600 were almost indistinguishable in solutions of different concentrations of K_2SO_4, and the obtained intrinsic viscosities were nearly the same in these solvents. However, the relative viscosity and intrinsic viscosity of PEG-35000 in aqueous solution decreased with increasing concentrations of K_2SO_4. The worsening quality of the solvent upon adding K_2SO_4 to aqueous PEG solutions led to decreases in the intrinsic viscosity of PEG-35000 with a size above the thermal blob size, while the size of PEG-600 was smaller than the thermal blob size, and the intrinsic viscosity was independent of the solvent quality. This result agrees with the molecular weight and K_2SO_4 concentration dependencies of the excluded volume exponent ν, as obtained from QCM-D (Fig. 8), which took the value of 0.5 for PEG with $M_w < 2000$ and decreased with increasing K_2SO_4 concentration in the high-M_w limit. The intrinsic viscosities of PEG in aqueous solutions containing different concentrations of K_2SO_4 are plotted as a function of molecular weight in Fig. 10. The reference data for PEG/PEO in water and 0.45 mol/L K_2SO_4 are also shown [39, 40, 44–47], which gave the Mark–Houwink relation $[\eta] = KM_w^{\alpha}$ with $K = 0.0308$ mL/g and $\alpha = 0.705 \pm 0.01$ in pure water, and $[\eta]_\theta = K_\theta M_w^{\alpha_\theta}$ with $K_\theta = 0.163$ mL/g and $\alpha_\theta = 0.50 \pm 0.01$ in 0.45 mol/L K_2SO_4. Our data for PEG in pure water and 0.43 mol/L K_2SO_4 are in excellent agreement with these data. The data for PEG in 0.19 mol/L K_2SO_4 were slightly lower than those for PEG in water, and the data for PEG in 0.57 mol/L K_2SO_4 were slightly lower than those at theta condition. Fits of the data to the relation $[\eta] = KM_w^{\alpha}$ in a limited molecular range of $5000 \le M_w \le 35{,}000$ led to $\alpha = 0.69 \pm 0.02$ in 0.19 mol/L K_2SO_4 and $\alpha = 0.45 \pm 0.01$ in 0.57 mol/L K_2SO_4. The variation of α for PEG/PEO in aqueous solutions containing different concentrations of K_2SO_4 agree well with the above results of the excluded volume exponent ν obtained by QCM-D, by considering the relation $\alpha = 3\nu - 1$.

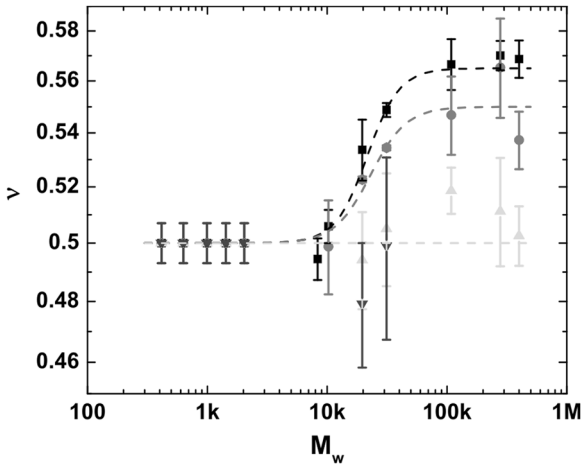

Fig. 8 The excluded volume scaling exponent ν as a function of the molecular weight of PEG/PEO samples in water (squares) and aqueous solutions containing different amounts of K_2SO_4: 0.19 mol/L (circles), 0.43 mol/L (upward triangles), and 0.57 mol/L (downward triangles). The dashed lines are guides to the eyes

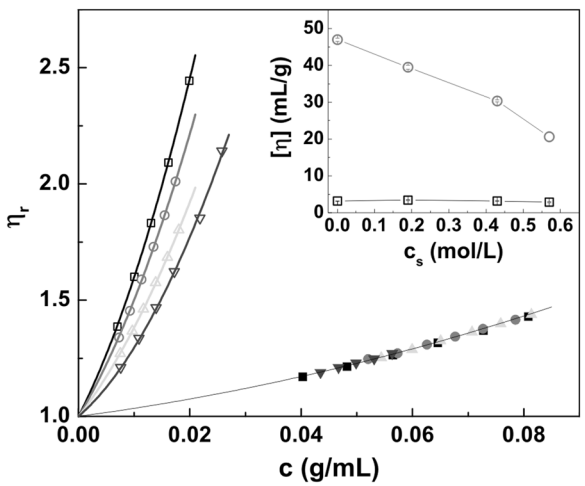

Fig. 9 Concentration dependence of the relative viscosities of PEG-600 (solid symbols) and PEG-35000 (open symbols) in water (squares) and aqueous solutions containing different amounts of K_2SO_4: 0.19 mol/L (circles), 0.43 mol/L (upward triangles), and 0.57 mol/L (downward triangles). The lines are fits to the data according to the Huggins plot: $\eta_r = 1 + [\eta]c + k_H[\eta]^2c^2$. The inset shows the dependence of the intrinsic viscosity $[\eta]$ on the K_2SO_4 concentration c_s

The viscoelasticity of 2% PEG/PEO aqueous solutions was also measured by a conventional rheometer at frequencies ω between 2 and 500 rad/s. However, no reliable complex-valued viscosity can be obtained for PEG with $M_w \leq 35{,}000$ at all. For PEO samples with the highest M_w of 116,000, 278,000, and 443,000, the dynamic viscosities can be obtained according to their agreement with the steady flow viscosities via the Cox-Merz rule [48]. However, no storage viscosity data could be obtained because the frequency range covered by the rheometer was $\omega \ll \tau^{-1}$. Fig. 11 shows the shear moduli of 2% PEO-116000 in water

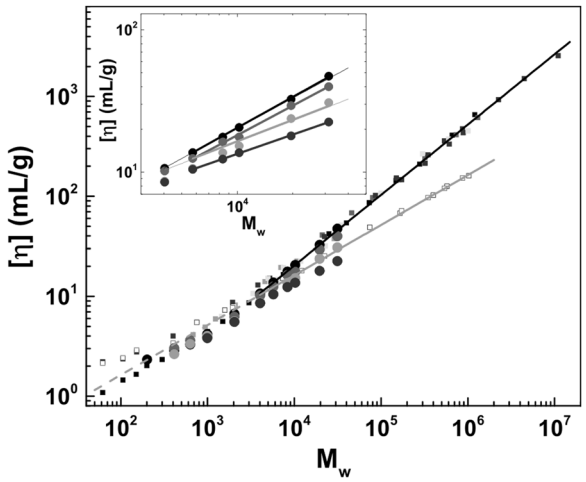

Fig. 10 Intrinsic viscosities of PEG/PEO in water (black solid circles) and aqueous solutions containing different amounts of K_2SO_4: 0.19 mol/L (red solid circles), 0.43 mol/L (green solid circles), and 0.57 mol/L (blue solid circles). The inset shows the fits to these data with exponents of 0.72, 0.69, 0.50, and 0.45. The intrinsic viscosity data in references [39, 40, 44–47] are also shown for PEG/PEO in a good solvent of water (solid squares) and in a theta solvent of 0.45 mol/L K_2SO_4 at 35 °C (open squares). The black and green lines are fits to all data with $M_w > 5000$: $[\eta] = KM_w^{\alpha}$ with $K = 0.0308$ mL/g and $\alpha = 0.705$ for PEG/PEO in water, and $[\eta]_\theta = K_\theta M_w^{\alpha_\theta}$ with $K_\theta = 0.163$ mL/g and $\alpha_\theta = 0.50$ for PEG/PEO in 0.45 mol/L K_2SO_4, respectively. The dashed green line is an extrapolation to the low-M_w region for the fit to the theta solvent

obtained from both QCM-D and the rheometer. The viscoelastic properties of this sample were obtained in the high-frequency region via QCM-D and in the low-frequency region by the rheometer. Both datasets are close to the Zimm model predictions of the shear moduli for dilute solutions of linear polymer chains, according to eqs. (7) and (8). As shown in the inset of Fig. 11, the dynamic viscosities η' of PEG/PEO solutions obtained via QCM-D agreed with the shear viscosity η obtained by the rheometer for low-M_w PEG but deviated significantly from that for high-M_w PEG/PEO, suggesting a crossover from Newtonian to non-Newtonian behavior with increasing molecular weight. It should be noted that the dynamic viscosity η' of PEG/PEO solutions were obtained from QCM-D at extremely high frequency and were substantially smaller than the values obtained by the rheometer working at low frequency.

Therefore, the viscoelastic properties of aqueous PEG solutions containing different concentrations of K_2SO_4 were successfully measured by QCM-D at megahertz frequency and were justified by conventional methods of viscometry and rheometry. The viscoelasticity of PEG solutions was probed by QCM-D over a broad normalized frequency range $\omega\tau$ between 10^{-2} and 10^4 by using a series of samples of different molecular weights. Newtonian behavior was observed for low-M_w PEGs, while non-Newtonian behavior was found for high-M_w PEGs. The high-frequency

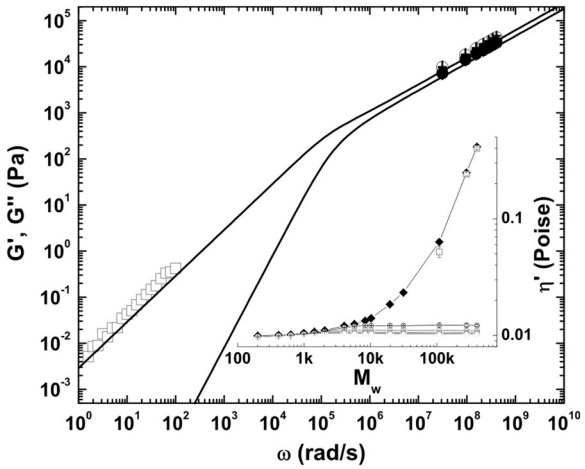

Fig. 11 Shear moduli of 2% PEO-116000 in water obtained from QCM-D for the loss modulus (open circles) and the storage modulus (solid circles) and from the rheometer for the loss modulus (open squares). The solid curves are the Zimm model predictions according to eqs. (7) and (8). The inset shows the dynamic viscosity η' of all 2.0% PEG/PEO aqueous solutions obtained from QCM-D with overtone numbers $n = 1, 3, 5, 7, 9, 11, 13$ (open circles from top to bottom) and by the rheometer (open squares). The steady flow viscosities obtained by the rheometer are also shown as solid diamonds

characteristic of QCM-D makes it possible to directly study the viscoelasticity of polymer solutions in a low-viscosity solvent, without the employment of time-temperature superposition. Thus the QCM-D technique is complementary to conventional rheometers working at low frequency. The QCM-D method might be useful for the viscoelasticity measurement of precious biomacromolecule samples, such as proteins, peptides, and nucleic acids. These biomacromolecules are usually studied in buffers containing different amount of salts, and their chain flexibility and conformation are controlled by the amount of added salts. It should be noted that to measure the solution viscoelasticity via QCM-D, one has to passivate the resonator by an inert layer, such as the SLB, which must be stable and nonadsorbing in the presence of the studied sample solutions.

Conclusions

The viscoelastic properties of PEG solutions in 0.19, 0.43, and 0.57 mol/L K_2SO_4 were studied by QCM-D after coating the resonator with a rigid SLB, which does not adsorb PEG molecules in aqueous solutions of K_2SO_4. The obtained results agree well with the Zimm model predictions in a good solvent and a theta solvent. The excluded volume exponent ν for high-M_w PEG decreased with increasing K_2SO_4 concentration, i.e., from 0.565 in water to 0.55 in 0.19 mol/L K_2SO_4, and 0.50 at higher K_2SO_4 concentrations, indicating the gradual worsening of solvent quality by adding K_2SO_4 to aqueous solutions of PEG. The excluded volume of larger PEG chains decreased with increasing K_2SO_4 concentration in aqueous solutions, as confirmed by decreases in the intrinsic viscosity as well as the Mark–Houwink exponent α.

Acknowledgements This work was supported by the Partner Group Program of the Max Planck Society and the Chinese Academy of Sciences, and the National Natural Science Foundation of China (21774125). YL wishes to acknowledge Dr. Bartosz Rozycki and Dr. Yani Zhao at the Institute of Physics, Polish Academy of Sciences and Dr. Quan Chen at the Changhun Institute of Applied Chemistry, Chinese Academy of Sciences, for enlightening discussions.

Compliance with ethical standards

Conflict of interest The authors declare that they have no conflict of interest.

Publisher's note: Springer Nature remains neutral with regard to jurisdictional claims in published maps and institutional affiliations.

References

1. Ferry JD. Viscoelastic properties of polymers. New York: Wiley; 1980.
2. Larson RG. The structure and rheology of complex fluids. New York: Oxford University Press; 1999.
3. Perkins TT, Smith DE, Chu S. Single polymer dynamics in an elongational flow. Science. 1997;276:2016–21.
4. Groisman A, Steinberg V. Elastic turbulence in a polymer solution flow. Nature. 2000;405:53–5.
5. Liu Y, Jun Y, Steinberg V. Concentration dependence of the longest relaxation times of dilute and semi-dilute polymer solutions. J Rheol. 2009;53:1069–85.
6. Rouse PE. A theory of the linear viscoelastic properties of dilute solutions of coiling polymers. J Chem Phys. 1953;21:1272–80.
7. Zimm BH. Dynamics of polymer molecules in dilute solution: viscoelasticity, flow birefringence and dielectric loss. J Chem Phys. 1956;24:269–78.
8. Morse DC. Viscoelasticity of concentrated isotropic solutions of semiflexible polymers. 2. Linear response. Macromolecules. 1998;31:7044–67.
9. Doi M, Edwards SF. The theory of polymer dynamics. Oxford: Clarendon Press; 1986.
10. Mason WP. Piezoelectric crystals and their applications to ultrasonics. Princeton: Van Nostrand; 1948.
11. Stokich TM, Radtke DR, White CC, Schrag JL. An instrument for precise measurement of viscoelastic properties of low viscosity dilute macromolecular solutions at frequencies from 20 to 500 kHz. J Rheol. 1994;38:1195–1210.
12. Yoshizaki H. Measurement of viscoelastic properties of polymer-solutions by torsional crystals. Polym J. 1993;25:553–9.
13. Fritz G, Pechhold W, Willenbacher N, Wagner NJ. Characterizing complex fluids with high frequency rheology using torsional resonators at multiple frequencies. J Rheol. 2003;47:303–19.
14. Dasgupta BR, Tee SY, Crocker JC, Frisken BJ, Weitz DA. Microrheology of polyethylene oxide using diffusing wave spectroscopy and single scattering. Phys Rev E. 2002;65:051505.
15. Del Guidice F, Tassieri M, Oleschlaeger C, Shen AQ. When microrheology, bulk rheology, and microfluidics meet: broadband

rheology of hydroxyethyl cellulose water solutions. Macroolecules. 2017;50:2951–63.
16. Zhao Z, Ji X, Lipowsky R, Dimova R, Liu Y. Viscoelasticity of poly(ethylene glycol) solutions on supported lipid bilayers via quartz crystal microbalance with dissipation. Macromolecules. 2015;48:1824–31.
17. Cho NJ, Frank CW, Kasemo B, Höök F. Quartz crystal microbalance with dissipation monitoring of supported lipid bilayers on various substrates. Nat Protoc. 2010;5:1096–1106.
18. Keller CA, Kasemo B. Surface specific kinetic of lipid vesicle adsorption measured with a quartz crystal microbalance. Biophys J. 1998;75:1397–1402.
19. Sauerbrey G. Verwendung von schwingquarzen zur wagung dunner schichten und zur mikrowagung. Z Phys. 1959;155:206–22.
20. Kanazawa KK, Gordon JG. Frequency of a quartz microbalance in contact with liquid. Anal Chem. 1985;57:1770–1.
21. Kanazawa KK, Gordon JG. The oscillation frequency of a quartz resonator in contact with a liquid. Anal Chim Acta. 1985;175:99–105.
22. Rodahl M, Kasemo B. On the measurement of thin liquid overlayers with the quartz-crystal microbalance. Sens Actuators A Phys. 1996;54:448–56.
23. Saluja A, Kalonia DS. Measurement of fluid viscosity at microliter volumes using quartz impedance analysis. AAPS PharmSciTech. 2004;5:68–81.
24. Johannsmann D. Viscoelastic, mechanical, and dielectric measurements on complex samples with the quartz crystal microbalance. Phys Chem Chem Phys. 2008;10:4516–34.
25. Johannsmann D. The quartz crystal microbalance in soft matter research: fundamentals and modeling. Berlin: Springer; 2015.
26. Voinova MV, Rodahl M, Jonson M, Kasemo B. Viscoelastic acoustic response of layered polymer films at fluid-solid interfaces: continuum mechanics approach. Phys Scr. 1999;59:391–6.
27. Richter RP, Brisson AR. Following the deformation of supported lipid bilayers on mica: a study combining AFM, QCM-D, and ellipsometry. Biophys J. 2005;88:3422–33.
28. Richter RP, Berat R, Brisson AR. Formation of solid-supported lipid bilayers: An integrated view. Langmuir. 2006;22:3497–505.
29. Jackman JA, Choi JH, Zhdanov VP, Cho NJ. Influence of osmotic prossure on adhesion of lipid vesicles to solid supports. Langmuir. 2013;29:11375–84.
30. Andrecka J, Spillane KM, Ortega-Arroyo J, Kukura P. Direct observation oand control of supported lipid bilayer formation with interferometric scattering microscopy. ACS Nano. 2013; 7:10662–70.
31. Kim M, Vala M, Ertsgaard CT, Oh SH, Lodge TP, Bates FS, et al. Surface plasmon resonance study of the binding of PEO−PPO −PEO Triblock copolymer and PEO homopolymer to supported lipid bilayers. Langmuir. 2018;34:6703–12.
32. Seifert U, Lipowsky R. Adhesion of vesicles. Phys Rev A. 1990;42:4768–71.
33. Jones G, Colvin JH. The viscosity of solutions of electrolytes as a function of the concentration VII silver nitrate, potassium sulfate and potassium chromate. J Am Chem Soc. 1940;62:338–40.
34. Hofmeister F. Zur lehre von der wirkung der salze. Arch Exp Pathol Pharmakol. 1888;24:247–60.
35. Boucher EA, Hines PM. Effects of inorganic salts on properties of aqueous poly(ethylene oxide) solutions. J Polym Sci Polym Phys. 1976;14:2241–51.
36. Dumetz AC, Lewus RA, Lenhoff AM, Kaler EW. Effects of ammonium sulfate and sodium chloride concentration on PEG/protein liquid-liquid phase separation. Langmuir. 2008; 24:10345–51.
37. Devanand K, Selser JC. Asymptotic behavior and long-range interactions in aqueous solutions of poly(ethy1ene oxide). Macromolecules. 1991;24:5943–7.
38. Li Q, Zhao Z, Zhao W, Ji X, Bo S, Liu Y. Band broadening and chain conformation of polyethylene oxide by gel permeation chromatography coupled with multi-angle laser light scattering. Chem J Chin Univ. 2016;37:761–6.
39. Kawaguchi S, Imai G, Suzuki J, Miyahara A, Kitano T, Ito K. Aqueous solution properties of oligo- and poly(ethylene oxide) by static light scattering and intrinsic viscosity. Polymer. 1997; 38:2885–91.
40. Beech DR, Booth C. Unperturbed dimensions of poly(ethylene oxide). J Polym Sci Part A-2. 1969;7:575–86.
41. Dittmore A, McIntosh DB, Halliday S, Saleh OA. Single-molecule elasticity measurements of the onset of excluded volume in poly(ethylene oxide). Phys Rev Lett. 2011;107:148301.
42. Lee H, de Vries AH, Marrink SJ, Pastor RW. A coarse-grained model for polyethylene oxide and polyethylene glycol: Conformation and hydrodynamics. J Phys Chem B. 2009; 113:13186–94.
43. Rubinstein M, Colby RH. Polymer physics. New York: Oxford University Press; 2003.
44. Kuga S. Pore size distribution analysis of gel substances by size exclusion chromatography. J Chromatogr. 1981;206:449–61.
45. Kato T, Nakamura K, Kawaguchi M, Takahashi A. Quasielastic light scattering measurements of polystyrene latices and conformation of poly(ethylene oxide) adsorbed on the latices. Polym J. 1981;13:1037–43.
46. Sun H, Cheng R. The viscositic property of polyethylene glycol solution. Chem J Chin Univ. 1995;16:467–70.
47. Armstrong JK, Wenby RB, Meiselman HJ, Fisher TC. The hydrodynamic radii of macromolecules and their effect on red blood cell aggregation. Biophys J. 2004;87:4259–70.
48. Cox WP, Merz EH. Correlation of dynamic and steady flow viscosities. J Polym Sci. 1958;28:619–22.